C. R. Geoscience 349 (2017) 391–401

Contents lists available at ScienceDirect

Comptes Rendus Geoscience

www.sciencedirect.com

Hydrology, Environment

Pockmarks on the South Aquitaine Margin continental slope: The seabed expression of past fluid circulation and former bottom currents

Guillaume Michel [a,*], Stéphanie Dupré [a], Agnès Baltzer [b], Axel Ehrhold [a], Patrice Imbert [c], Mathilde Pitel [a], Benoît Loubrieu [a], Carla Scalabrin [a], Pascal Lazure [d], Louis Marié [d], Jean-Baptiste Geldof [e], Éric Deville [f]

[a] IFREMER – unité Géosciences marines, 29280 Plouzané, France
[b] CNRS, UMR 6554, Université de Nantes, 44312 Nantes cedex 3, France
[c] TOTAL, Centre scientifique et technique Jean-Féger, avenue Larribau, 64018 Pau cedex, France
[d] IFREMER, laboratoire d'Océanographie Physique et Spatiale, 29280 Plouzané, France
[e] TOTAL, 10, place des Vosges, 92072 Paris-La-Défense, France
[f] IFPEN, 1 et 4, avenue de Bois-Préau, 92852 Rueil-Malmaison, France

ARTICLE INFO

Article history:
Received 13 July 2017
Accepted after revision 9 October 2017
Available online 7 December 2017

Handled by Isabelle Manighetti

Keywords:
Pockmark
Fluid
Seabed morphology
Aquitaine slope
GIS
Currents

ABSTRACT

Inactive and mostly elongated pockmarks of 100–200 m in dimension were recently discovered on the South Aquitaine Margin continental slope. They are distributed at water depths greater than 350 m in both interfluve and sediment-wave areas, and are strongly controlled by the sedimentary morphology and architecture. Water column and seafloor backscatter and sub-bottom profiler data do not exhibit present-day or past gas evidence, e.g., massive and continuous gas releases at the seabed and fossil methane-derived authigenic carbonates. It is thus proposed that the pockmarks originated from a shallow source and result from relatively recent and short-duration gas or water expulsion events. Former near-bottom currents may have contributed to the elongation of these WNW–ESE-oriented pockmarks, whereas present-day weaker near-bottom currents may induce upwelling, contributing to the maintenance of the elongated shapes of the pockmarks.
© 2017 Académie des sciences. Published by Elsevier Masson SAS. This is an open access article under the CC BY-NC-ND license (http://creativecommons.org/licenses/by-nc-nd/4.0/).

1. Introduction

Pockmarks were first described by King and MacLean (1970) as seafloor morphological depressions, formed by fluid escapes. Pockmarks are commonly encountered and, are worldwide, related to fluid migrating upward (Judd and Hovland, 2007) and triggering-sediment resuspension during leakage and sediment collapse. These depressions are observed from shallow environments (Rise et al., 2015) to deep bathyal environments (Gay et al., 2006). Pockmark morphologies can be associated with various types of fluids and processes, e.g., small-scale pockmarks can be related to a unique local gas source (Gay et al., 2007), to dewatering of the sediments upon compaction (Harrington, 1985) and to freshwater seeps (Whiticar, 2002) while pluri-kilometre-scale pockmarks may indicate hydrate dissolution (Sultan et al., 2010). Pockmarks may occur as clusters (Hovland et al., 2010) or as strings of pockmarks (Pilcher and Argent, 2007). Strings of pockmarks are commonly related to geological features focusing fluid

* Corresponding author.
E-mail address: guillaume.michel@ifremer.fr (G. Michel).

https://doi.org/10.1016/j.crte.2017.10.003
1631-0713/© 2017 Académie des sciences. Published by Elsevier Masson SAS. This is an open access article under the CC BY-NC-ND license (http://creativecommons.org/licenses/by-nc-nd/4.0/).

flows, e.g., fractures and faults (Gay et al., 2007) and buried valleys (Baltzer et al., 2014).

The modification of the original pockmark morphologies will depend on internal factors such as successive fluid expulsion events (Judd and Hovland, 2007), the presence of methane-derived authigenic carbonates (Gay et al., 2006), and external factors such as bottom currents (Bøe et al., 1998; Josenhans et al., 1978; Schattner et al., 2016), slumping and sedimentary destabilization along the slope direction (Brothers et al., 2014), presence of benthic fauna and debris accumulation (Webb et al., 2009), e.g., coarser sediments (Pau and Hammer, 2013). Bottom currents may contribute to elongate pockmarks along the direction of the currents by eroding sediments and preventing sedimentation over the pockmarks (Andresen et al., 2008; Dandapath et al., 2010). Bottom currents may induce upwelling within the pockmarks that would limit the sedimentation of fine-grained sediments, therefore maintaining pockmark morphology (Brothers et al., 2011; Hammer et al., 2009; Pau et al., 2014). Moreover, coalescent pockmarks (merging depressions) (Gay et al., 2006) may be a result of successive fluid escapes or external processes as cited above, eventually forming elongated pockmarks. Pockmark morphological characteristics, accessible through their acoustic signature, may be used to determine potential activity (Dupré et al., 2010; Hovland et al., 2010), and the nature of fluids involved (Gay et al., 2006; Judd and Hovland, 2007) and also to address the relative timing of pockmark formation with regards to surrounding sedimentation (Bayon et al., 2009).

The present study mainly focuses on the geophysical characterization of a wide pockmark field discovered on the continental slope of the Aquitaine Margin (offshore France) in 2013 during the GAZCOGNE1 oceanographic expedition. Pockmark activity and the nature of fluids involved in pockmark formation are discussed. Particular attention is paid to the pockmark reshaping related to external factors such as bottom currents.

2. The setting

Related to the opening of the North Atlantic Ocean, the Bay of Biscay initially corresponded to a V-shaped rift, initiated during the Late Jurassic and aborted in the mid-Upper Cretaceous (Roca et al., 2011). Its extensional phase was stopped during the Santonian age by the opening of the South Atlantic Ocean. The subsequent northward drift of the Iberian plate and the related compression phase led to the Pyrenean orogeny (Roca et al., 2011). The Bay of Biscay is surrounded by different shelves, the large Armorican Shelf, the Aquitaine Shelf, the Basque Shelf, and the Iberian Shelf (Fig. 1) with a major morphological high, the Landes Plateau. The hydrocarbon Parentis Basin, created during the Pyrenean Orogeny, extends from the onshore to the offshore domain, in the southern part of the Aquitaine Shelf (Biteau et al., 2006) (Fig. 1).

The study area is located in the French EEZ (Exclusive Economic Zone) on the continental slope of the Aquitaine Shelf, from 200 m to 1600 m water depths, with a mean smooth slope of ~3° (Figs. 1 and 2). This area is 60–80 km westward of the coastline, between the Cap Ferret Canyon

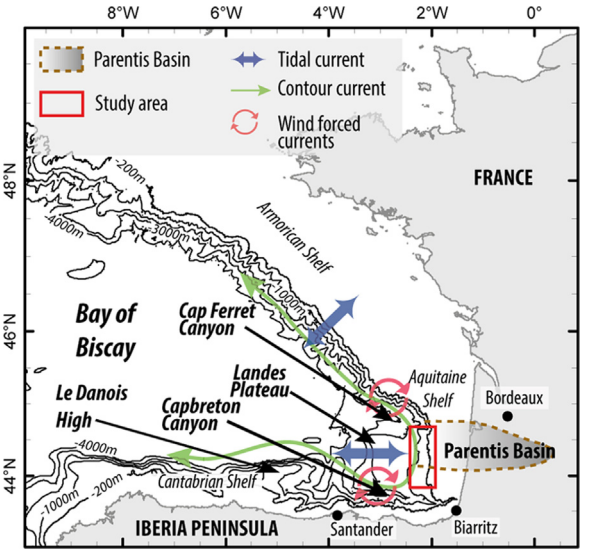

Fig. 1. Synthetic map of the Bay of Biscay with indication of the main current regimes (see references therein) and main isobaths (Sibuet et al., 2004). The study area (red rectangle) covers the western extension of the Parentis Basin (Biteau et al., 2006) and the eastern Landes Plateau.

(44°40′N) and the Cap breton Canyon (43°30'N). The study area can be divided into two main morphological domains. The northern part, from 44°35′50″N to 44°11′44″N of latitude, is deeply incised by east–west-oriented canyons with heads rooted at the shelf-break edge. There, the inter-canyon areas are kilometer-wide along the north–south axis (Fig. 2a) and are affected by slope instabilities within a context of silt dominated sedimentation (Schmidt et al., 2014). The southern part, from 44°11′44″N to 43°52′37″N of latitude, does not show any canyons, only some landslide scarps located at 230 m in water depth and a wide sediment-wave field located between 250 and 1000 m in water depth (Fig. 2), with a surficial sandy silt sedimentation, extending from the shelf break to the foot slope (Faugères et al., 2002; Gonthier et al., 2006). Sediment wave morphologies, with wavelengths between 800 m and 1600 m and heights from 20 m to 70 m show crests slightly oriented at an oblique angle of the main slope, between 010°N and 035°N. The influence of bottom currents in the formation processes of sedimentary waves along the Aquitaine slope has been indicated (Faugères et al., 2002; Gonthier et al., 2006). The sedimentary waves are covered by a thin homogenous layer corresponding to the U4 unit described by Faugères et al. (2002), which is 12–15 m in thickness (Gonthier et al., 2006) and pinches out on the upper slope between 400 and 300 m water depth. The surficial sedimentary cover of the Aquitaine Shelf is mainly composed of sand and silty sand (Cirac et al., 2000). Inactive pockforms and pockmarks have been described on the Landes Plateau (Baudon et al., 2013; Iglesias et al., 2010) and on the Basque Shelf (Gillet et al., 2008), respectively. Recently, Dupré et al. (2014a) described an active cold seep system at the edge of the Aquitaine Shelf without any pockmarks.

The hydrography regime of the study area appears to be complex, due to the semi-enclosed morphology of the

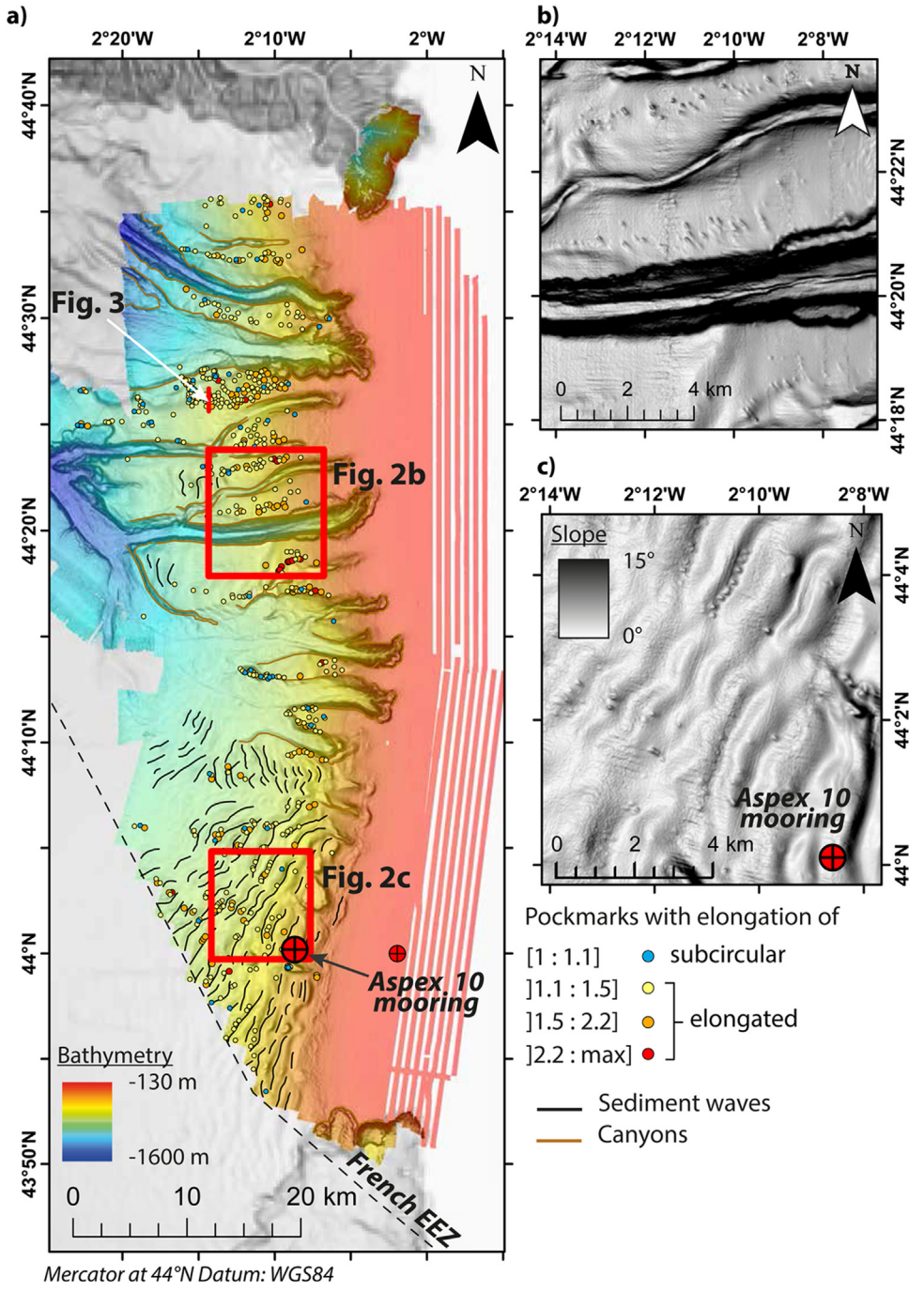

Fig. 2. (a) Detailed shaded bathymetry map of the Aquitaine Margin with main seafloor morphologies: pockmarks, canyons and sediment waves. Background bathymetry from EMODnet Bathymetry portal (http://www.emodnet-bathymetry.eu). ASPEX 10 current mooring is located at a water depth of 450 m in the sediment-wave field. Slope focus on (b) elongated pockmarks in the northern inter-canyon area and (c) subcircular pockmarks in the sediment-wave field.

Bay of Biscay and the interaction between different currents of different time scales, meso-tidal currents (Batifoulier et al., 2012; Charria et al., 2013; Le Boyer et al., 2013), contour currents (Van Aken, 2000), and some temporary currents related to wind-forced events (Kersalé et al., 2016).

3. Data and methods

3.1. Geophysical data acquisition and processing

High-resolution marine geophysical data were acquired during the BOBGEO2 expedition in 2010 and more

significantly during the GAZCOGNE1 survey in 2013 covering 3200 km^2 of the seafloor at water depths ranging from 130 m to 1600 m (Fig. 2). During the GAZCOGNE1 survey, multibeam bathymetry, water column and seafloor backscatter and seismic reflection (sub-bottom profiler) data were acquired simultaneously. Multibeam data were collected onboard the R/V Le Suroît with a Kongsberg EM302 ship-borne multibeam echosounder operated at a frequency of 30 kHz with the celerity profile calibrated with ©Sippican shots. Seafloor multibeam data were processed through CARAIBES software (©IFREMER) with application of bathymetric filters and correction of position, pitch, roll and tide effects for raw bathymetric data and with the generation of a compensation curve to harmonize values along the survey lines for seafloor backscatter data. Both bathymetry and seafloor backscatter processed data were mainly exported to mosaic grids of 15×15 m (with some backscatter maps at 10×10 m cells). Water column backscatter data only recorded during the GAZCOGNE1 marine expedition were processed in SonarScope software (©IFREMER) and then interpreted in GLOBE/3DViewer (©IFREMER) (Dupré et al., 2015).

The sub-bottom profiles were recorded with the ship-borne sub-bottom profiler ECHOES 3500 ©T7iXblue emitting a linear frequency modulated signal, ranging from 1.8 to 5.3 kHz, with a vertical resolution of 10 cm and a maximum vertical penetration of 100 m. A 2D sub-bottom profiler insonifies a surface at the seafloor defined by the Fresnel equation and may record lateral reflexions from close-by 3D features, as well as artefacts. These artefacts may be displayed as diffraction hyperbola (Dupré et al., 2014b) and triplication points, so-called "bow ties" (Moss et al., 2012). Raw data were processed with QC-SUBOP software (©IFREMER) before being exported in SEG-Y and then interpreted in ©Kingdom software (Fig. 3).

The water current data were acquired during the ASPEX2010A mooring survey (Le Boyer et al., 2013) with an Acoustic Doppler Current Profiler (ADCP) operated at a frequency of 75 kHz and recording every 2 minutes. The data discussed in this paper come from mooring 10 located at 44°00′4.1″N–02°08′38.6″W at 450 m water depth in the sediment-wave field (Figs. 2a and c). Water current data were recorded over more than 6 months (18th July 2009–30th January 2010). Current velocities were integrated between 17 m and 33 m above the seafloor and averaged every 20 min. Classic harmonic tide analyses were conducted on ASPEX current data to extract tide-related signals from the raw signal (Lazure et al., 2009).

3.2. Pockmark morphometry

All pockmarks were manually delimitated, identified by their rim on the slope grid (processed at 15 m and calculated with Slope function in Spatial Analyst toolbox from Arcmap 10.2, ©ESRI). It is worth noting that below the bathymetry resolution (15 m), detection cannot be performed effectively. In other words, small pockmarks of diameter < 30 m, if present, could not have been mapped.

Eleven morphological attributes were extracted from GIS for each pockmark: its area, perimeter, area/perimeter ratio, internal depth (from the rim down to the apex of the pockmark), minor and major axis lengths, major axis direction, elongation (major/minor axis length ratio), bathymetry, slope within the pockmark and morphological domain. The morphological attributes of the Aquitaine slope pockmarks are available online as a SEANOE public

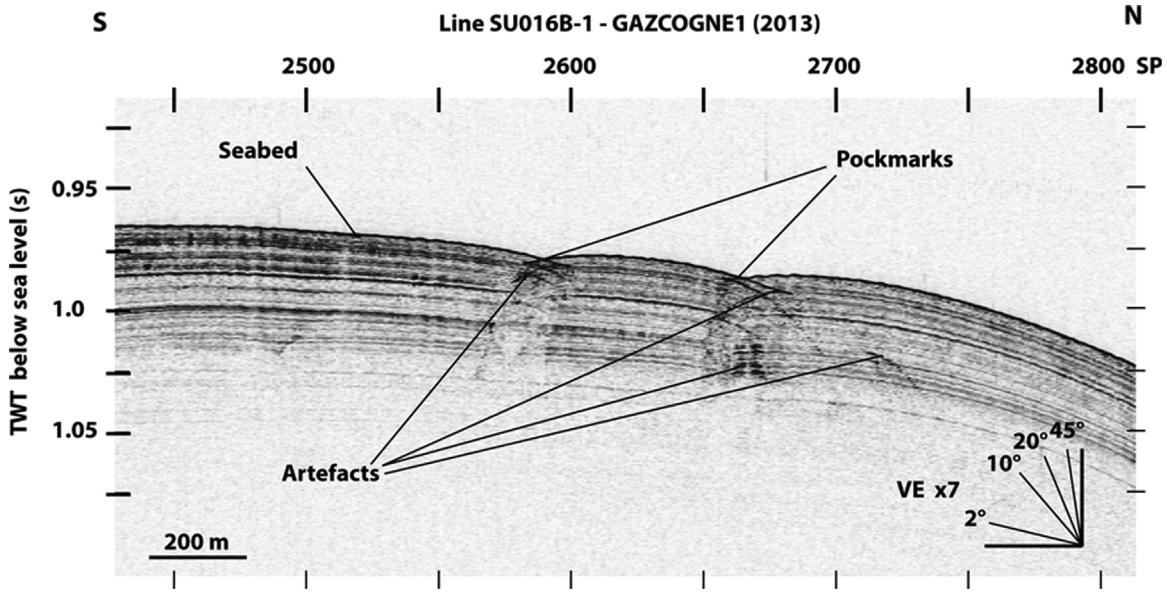

Fig. 3. Processed sub-bottom profiler line displayed in envelope in ©Kingdom Software. X-axis corresponds to Shot Point (SP) and Y-axis to depth in seconds in Two Way Time (TWT). The profile is displayed with a Vertical Exaggeration (VE) of 7, calculated with a seismic wave velocity of 1500 m/s, with indication of slope angle. This sub-bottom profiler line crosses two pockmarks (see location in Fig. 2a) without any fluid evidence and exhibits only triplication points, so-called "bow tie" artefacts.

database with information on pockmark location and seafloor backscatter data (Michel et al., 2017). Complementary information on morphometric methods is available online (Appendix A, supplementary text).

4. Results

4.1. Pockmark spatial distribution

Six hundred and six pockmarks were discovered, exclusively located on the continental slope, from 350 m water depth in the upper slope down to 1150 m water depth, covering 800 km^2 (Fig. 2). The oceanward extension of the pockmarks is limited by the survey acquisition (Fig. 2). The mapped pockmarks are relatively large, with regards to known pockmarks (Judd and Hovland, 2007; Pilcher and Argent, 2007), with a rough diameter from 52 to 330 m and an internal depth up to 42 m for the largest pockmarks (Fig. 4a). The majority of the pockmarks (80%) have a rough diameter between 100 and 200 m for an average internal depth of 15 m (Appendix A, supplementary figure 1).

Seventy-two percent (434 units) of the pockmarks occur in the inter-canyon areas (574 km^2) and 25% (153 units) in the sediment-wave field (374 km^2) (Figs. 2 and 5). Pockmark density in the inter-canyon domain is twice as high as in the sediment-wave field. The 3% (19 units) remaining pockmarks are located deeper at the foot slope (Fig. 2). In the northern part of the studied area, the pockmarks are completely absent from the canyons. Confined within the inter-canyons, the pockmarks spread along an east–west direction. The pockmarks are distributed both at the summits of the antiforms (see, e.g., the second northern inter-canyon in Fig. 2) and at the borders of the canyons (see, e.g., the southern border of the inter-canyon at 44°17′N in Fig. 2). The majority of the pockmarks do not form alignments or so-called pockmark trains. Their distribution is more diffuse within each inter-canyon area

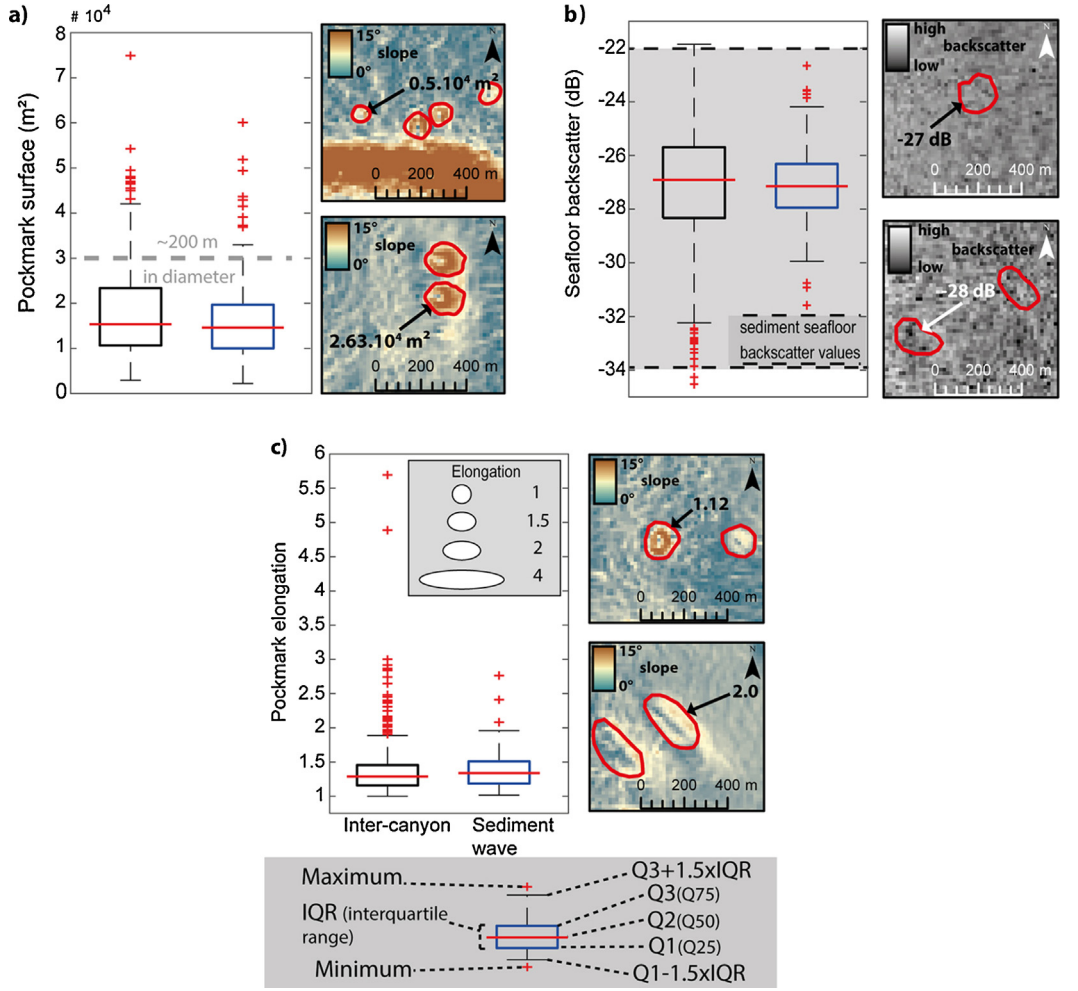

Fig. 4. Box plots of (a) pockmark area with indication of diameter with regards to pockmark surface (a circular pockmark with a diameter of 200 m corresponds to a surface of 3×10^4 m^2), (b) pockmark seafloor backscatter amplitude from the 30 kHz EM302 multibeam data and (c) pockmark elongation. Red curves in maps stand for the contour of pockmarks. The legend of the box plots is displayed in Fig. 4c, with representation of the minimum, maximum, first quartile (Q25), second quartile (Q50 or median), third quartile (Q75) of the series and series outliers.

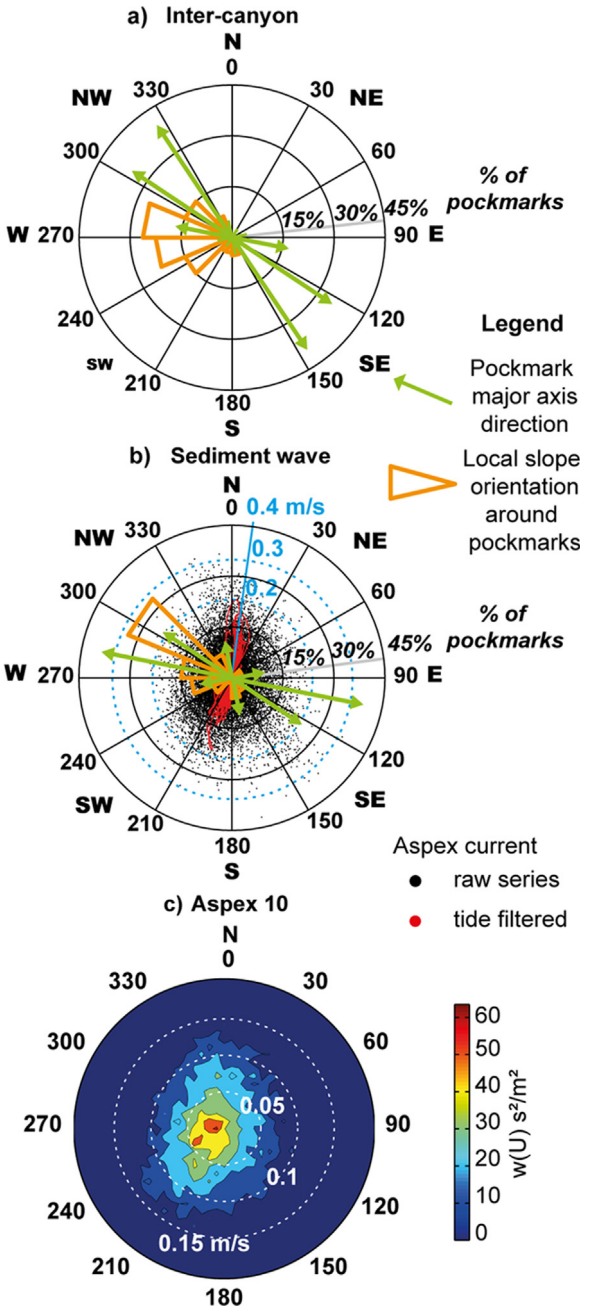

Fig. 5. Rose diagrams of the pockmark major axis direction and local slope direction around pockmarks for (a) inter-canyon and (b) sediment-wave areas. Arrow and shape lengths are proportional to the number of pockmarks involved. Recorded velocity and orientation of currents from ASPEX mooring 10 are shown in black and red dots for raw and tide-filtered data, respectively and (c) diagram of spatial distribution of current velocities and orientations of raw signals.

unless the inter-canyons are narrow (see, e.g., the inter-canyon at 44°13′N in Fig. 2). A few pockmark clusters are also observed (Fig. 2) with densities up to 12 pockmarks per km^2. Locally, a few coalescent pockmarks appear to form elongated pockmarks (Fig. 2b). In the sediment-wave field, pockmarks are located both on the wave crests (36%) and between the crests (48%), as noticed by Baudon et al. (2013) for similar pockmarks located on the upper slope of the Aquitaine slope south of the studied area. The 16% remaining pockmarks are located on relatively flat areas without any spatial organisation. Therefore, the main regional pockmark repartition in the sediment wave domain follows the sediment wave's crests and inter-crests direction between N010 and N035 (Figs. 2a and c) rather than an east–west direction. Locally, a few pockmark strings (maximum 8 depressions along 2 km), only concerning less than 13% of the 153 pockmarks mapped in the sediment-wave field, are observed related to sediment wave orientation (Figs. 2a and c). From the northern part of the sediment-wave field to the southern part, the pockmark density increases and pockmarks are also located deeper in the slope. Pockmarks are however absent from two main corridors crossing the sediment-wave field with a convergence and narrowing of the pockmark field downslope (see uppermost part of Fig. 2c).

4.2. Pockmark characterization

4.2.1. Acoustic signature of water column and surficial sediments

The EM302 water column backscatter data from the GAZCOGNE1 marine expedition do not exhibit any amplitude anomaly in the water column related to gas bubble escapes, and this throughout the pockmark field and over the six days of the acoustic survey (28th July to 2nd August 2013).

The average seafloor backscatter amplitude within the pockmarks (excluding 57 pockmarks located at the vertical of the ship track where the data are worthless) ranges from −34.5 to −21.8 dB in the inter-canyons with a mean value of −27.2 dB (Fig. 4b). The seafloor backscatter amplitude values varies from −31.6 to −22.6 dB with a mean value of −27.1 dB in the sediment-wave field (Fig. 4b). The seafloor backscatter of surrounding sediment, calculated within a 100 m buffer around the pockmark rim, varies from −34 dB to −23 dB with a mean value of −27 dB. The EM302 seafloor backscatter values in the majority of the pockmarks are similar to the ones of surficial sediments around wherever pockmarks are located in inter-canyon or sediment-wave field domains. Only a small percentage of the pockmarks exhibits, within part of the depression, high or low seafloor backscatter amplitudes that contrast with the surrounding seafloor.

4.2.2. Seismic investigation at the seabed and inside the sediment pile

The acquired sub-bottom profiler lines only cross 38 pockmarks. The profiles do not exhibit any high seafloor amplitude anomalies, e.g., enhanced reflectors, or high-amplitude anomalies within the uppermost 100 m of sediment (Fig. 3). Only triplication points due to geometry artefacts below pockmarks are observed. The sedimentary records below and besides the pockmarks are not disturbed. Moreover, no distinct draped sediment layers are observed within the depressions with regards to the ten centimetres resolution from the sub-bottom profiler.

4.2.3. Pockmark morphometry

The pockmark surface ranges from 0.29×10^4 m^2 to 7.49×10^4 m^2 at the inter-canyon area, and from 0.25×10^4 m^2 to 6×10^4 m^2 in the sediment-wave field area. The mean value of pockmark surface is 1.8×10^4 m^2 in the inter-canyon and 1.7×10^4 m^2 in the sediment-wave field (Fig. 4a). The variations in pockmark size are similar in both morphological domains. A general increase in pockmark surface is observed at shallower water depths but no linear trend is observed (regression line, $R^2 = 0.1259$ in the inter-canyon area and $R^2 = 0.1895$ in the sediment-wave field) (Appendix A, supplementary figure 1).

The pockmark internal depth ranges from 4 to 42 m with a mean value of 15 m (Appendix A, supplementary figure 1). The deepest internal depth values correspond to the largest pockmarks (> 200 m in diameter) with a mean value of 22 m.

The pockmark elongation ranges from 1 to 5.7 with a mean value of 1.4 on the inter-canyon area and from 1 to 2.7 with a mean value of 1.4 in the sediment-wave field (Fig. 4c). Most of the pockmarks (88%) are elongated with an elongation superior to 1.1 while only 12% are subcircular (elongation between 1 and 1.1) (Fig. 2). Elongation values < 1.1 are considered as subcircular shapes to take into account potential mapping biases and calculation approximation. Among the elongated pockmarks, a majority has an elongation between 1.1 and 1.5 (66%) while 19% have an elongation between 1.5 and 2.2. The most elongated pockmarks with an elongation > 2.2 are less common (3%) and mainly correspond to coalescent pockmarks (Fig. 2b, most southeastern pockmarks).

The major axis direction of the pockmarks with elongation values > 1.5 (134 units) has been compared to the surrounding slope value (Fig. 5). These pockmarks correspond to 92 depressions in the inter-canyon domain and 42 in the sediment-wave field. In the inter-canyon domain, local slope orientation around the pockmarks is mostly east–west, while the pockmark major axis is mostly NW–SE, with 40% of them oriented N150–330 and 35% others oriented N120–300. In the sediment-wave field, the local slope around the pockmarks is oriented around N300 and the pockmark major axes are mostly oriented WNW–ESE, 40% of them being oriented N100–280 and 22% oriented N120–300.

4.3. Bottom currents in the sediment-wave field

Current direction and amplitude distributions are displayed in current roses (Fig. 5) with east–west and north–south current components (Appendix A, supplementary figure 2). Current velocities derived from the raw signal are mostly lower than 10 cm/s (90% of the records for the east–west component and 81% for the north–south component) (Fig. 5c) with the maximum amplitude reaching 34 cm/s during two events, 10 days apart, over the six months of the acquisition. Currents vary on different time scales, associated with different forcing factors. A large-amplitude semi-diurnal tidal signal (current vector period close to 12 h, current amplitude period close to 6 h) coexists with weaker signals that have longer periods (approximately one week). The tidal signal is mostly oriented east–west, and exhibits a significant cross-slope component. The longer-period component (red curves in Appendix A, supplementary figure 2) is oriented along-slope due to the geostrophic constraint, as evidenced by the red dots in Fig. 5. Its cross-slope component is always smaller than 5 cm/s. The along-slope component is almost always weaker than the tidal current (for 81% of the records), but can reach high instantaneous values during specific events (higher than 15 cm/s, 6% of occurrence).

5. Discussion

5.1. Pockmark inactivity and nature of the fluids involved

Free gas leakage produces clear water column backscatter anomalies commonly used to attest to seepage activity (Dupré et al., 2015). During the GAZCOGNE1 survey, no water column acoustic anomalies corresponding to gas bubbles were detected in the whole slope area. Although the temporal variability of seepage activity may be invoked, the six days of the acoustic survey are sufficient to cover the time window for the tidal cycle, which could be a possible triggering mechanism (Baltzer et al., 2014). Thus, pockmarks along the Aquitaine slope are interpreted as currently inactive in terms of free gas seepage.

Considering the sediment cover, methane-derived authigenic carbonates are considered as confident indicators of long-term gas circulation (Bayon et al., 2009). Outcrops and sub-outcrops of carbonate structures are easily detected on seafloor backscatter data as occurrence of high amplitude anomaly patches (Dupré et al., 2010). The lack of high seafloor backscatter values within the pockmarks and the similarity of seafloor acoustic signature between the pockmarks and the surrounding sediments clearly provide evidence for the absence of methane-derived authigenic carbonates along the Aquitaine slope.

Within the uppermost 100 m of the sediment, sub-bottom profiles across pockmarks do not exhibit any enhanced reflectors and diffracting points at the seabed pile that carbonates would seismically produce if present (Dupré et al., 2010). No acoustic blanking, blank chimneys or any other seismic evidence of gas accumulations within the vertical resolution limit of ten centimetres are observed. At the present day, the absence of acoustic anomalies within sedimentary records excludes the occurrence of (1) layers charged with free gas, (2) buried pockmarks and (3) carbonates underlying or disconnected from the present-day seafloor pockmarks.

Based on these observations and interpretations, the pockmarks along the Aquitaine slope may have been formed by dewatering (Harrington, 1985), freshwater expulsion (Whiticar, 2002) or short-duration gas escapes, associated with a relatively shallow source level (the pockmarks being rooted a few metres to maximum a few tens of metres below the seafloor) (Judd and Hovland, 1992). Indeed, gas releases over a long period of time (order of kyr) would have led to authigenic carbonate

precipitation (Andresen et al., 2008). Although the pockmarks along the Aquitaine slope are located away from the hydrate stability zone, it is unlikely with regards to the absence of fluid evidence that they were formed by gas hydrate dissociation as suspected along the US Atlantic continental margin (Brothers et al., 2014). Moreover, the morphology and acoustic signature of the studied pockmarks do not fit those of hydrate–bearing pockmarks (Sultan et al., 2010). The latter are generally kilometre-large depressions with internal filling of disturbed sediments caused by hydrate destabilization. A few smaller pockmarks may be associated with these mega structures, but exhibit disturbed sediments underneath (Davy et al., 2010).

Based on sub-bottom profiler data displayed in Gonthier et al. (2006) and in accordance with the seismic signature of pockmarks from our dataset, we suspected the occurrence of pockmarks within the recent sedimentary cover, which corresponds in the sediment-wave field mainly to the so-called U4 unit (Faugères et al., 2002). This view is strengthened by the fact that above the pinch out of this unit U4 on the upper slope, roughly at water depth of 350 m, pockmarks are absent. This reinforces the shallow character (a few tens of metres maximum) of the Aquitaine slope pockmarks. The formation of the pockmarks appears therefore to postdate the sediment wave formation (U3 unit). Based on the age of the base of the 12–15 m thick U4 unit, which depends on the sediment rates, 10 cm/kyr (Winnock, 1973) or 100 cm/kyr (Schmidt et al., 2014, 2009), the pockmarks along the Aquitaine slope may have been initiated after 120–150 kyr BP or 12–15 kyr BP, respectively. Within this context, sea level falls may have triggered fluid escapes and initiation of pockmarks in the Aquitaine Basin, as evidenced e.g., in the Gulf of Lions (Riboulot et al., 2014) and offshore West Africa (Plaza-Faverola et al., 2011). But without any detailed seismic data and dating of long cores through the Aquitaine slope, it is impossible to conclude.

With regards to the available data and the inactivity, morphology and repartition of the studied Aquitaine pockmarks, there is no similarities with the other known, but not much documented, fluid systems of the Bay of Biscay: (1) the Cap breton Canyon area, where size-differentiated pockmarks are related to different migration pathways (Baudon et al., 2013; Gillet et al., 2008), (2) deeper offshore mega-pockforms on the Landes Plateau (Baudon et al., 2013; Iglesias et al., 2010) and (3) gas emissions on the Aquitaine Shelf (Dupré et al., 2014a).

5.2. Origin of pockmark elongation: slope, coalescence, currents?

As it is assumed that pockmarks initially have a subcircular shape (Judd and Hovland, 2007), why are the majority of the pockmarks (88%) located along the Aquitaine slope (deeper than 350 m water depth) elongated?

With regards to inactivity and the absence of present and past fluid evidence, it is unlikely that successive fluid releases have occurred, and even less unlikely that this was able to reshape the pockmarks. The slope along which pockmarks may become elongated and open downslope (Brothers et al., 2014) may be another explanation for pockmark elongation. This may apply to some pockmarks in the sediment-wave field area but cannot account for all the depressions, as the directions of the slope and of the elongated pockmarks are not compatible. Coalescence of several pockmarks may in places explain some of the most elongated pockmarks observed along the Aquitaine slope, especially in the northern part.

The influence of the bottom currents on pockmark morphology, namely their elongation, has been evidenced across other continental shelves (Schattner et al., 2016) and slopes (Tallobre et al., 2016), and is questioned here for the pockmarks along the Aquitaine slope. Current-induced processes that can produce strong shear stress on the seafloor, such as high-density flow on the slope (Kuhnt et al., 2013) and internal tide impacting the seabed (Pingree et al., 1986), may influence seafloor morphology. Along the Aquitaine slope, indirect evidence of benthic material resuspension has been observed (Durrieu De Madron et al., 1999; Kuhnt et al., 2013). The hypothesis put forward by Durrieu De Madron et al. (1999) regarding the resuspension mechanism is an intensification of internal tidal current shear close to the seabed, which happens to be tangent to the internal tide rays (Pingree et al., 1986) over extensive areas of this region (Kuhnt et al., 2013). Direct observations of this process are still lacking however, and it is thus hard to ascertain if this process is really dominant and if its intensity is sufficient to have an impact on seafloor morphology along the Aquitaine slope.

The present-day bottom current direction does not correspond to the elongation direction of the pockmarks along the Aquitaine slope. Two main current regimes are evidenced, one driven by the semi-diurnal tide and mostly oriented east-west, and a second long-period (period of a week) current mostly oriented north-south. In contrast, the pockmark elongation varies in direction from NW–SE to WNW–ESE for the inter-canyon area and sediment wave domain, respectively. Moreover, the 12% pockmarks, which are subcircular occurring randomly amidst elongated ones are not coherent with the influence of a regional bottom current.

Independently of the current direction, the velocity amplitudes of the bottom currents, mainly lower than 10 cm/s are not compatible with erosion. Current velocities of 10 cm/s are indeed sufficient to limit sedimentation for silt and mud (Migniot, 1977) therefore preventing pockmark filling. On the other hand, in order to remobilize consolidated silt, velocities higher than 30 cm/s are necessary (Migniot, 1977). Thus, most of the present-day tide velocity and north–south current velocity is not strong enough to remobilize sediment along the Aquitaine slope. However, some stronger current events associated with higher velocities, such as the ones observed reaching up to 34 cm/s in the along-slope S/N direction along the Aquitaine slope, may contribute over short timescales to remobilize sediments within the pockmarks. Yet the direction of these stronger bottom currents is not compatible with the direction of the elongated pockmarks. Along the Aquitaine slope, these stronger events are clearly associated with westerly-wind pulses occurring along the

Cantabrian Slope (Batifoulier et al., 2012). And the range of velocities recorded along the Aquitaine slope may induce regularly upwelling within the depressions preventing fine sediments from being deposited (Brothers et al., 2011; Hammer et al., 2009). This would not exclude the accumulation of coarser sediments within the pockmark as inferred from the high seafloor backscatter of some of the pockmarks.

Considering that circular pockmarks along the Aquitaine slope were formed at the same time, the post-formation processes that have reshaped and elongated the pockmarks along the WNW–ESE axis may be related to a former current regime that differs from the present-day one. At present-day, upwelling induced by near-bottom currents within the pockmarks may contribute to maintaining the depressions, preventing sedimentation by winnowing out the fine-grained sediments (Brothers et al., 2011; Hammer et al., 2009; Pau et al., 2014). Relatively weak near-bottom currents along the US Atlantic continental margin (< 20 cm/s), as with those along the Aquitaine slope, appear sufficient to induce such upwelling (Brothers et al., 2011). The few slightly elongated pockmarks (12%) corresponding to subcircular pockmarks may be explained by subsequent filling-in possibly caused by collapse within these former elongated pockmarks. It can be also considered that these subcircular pockmarks may have been formed after the formation and subsequent elongation by bottom currents of the initial majority of pockmarks.

6. Conclusion

The geophysical survey conducted on the Aquitaine slope revealed numerous pockmarks (606) over 800 km^2 occurring on canyon interfluves and in the southern sediment-wave field from water depths of 350 m within the upper slope to greater depths westwards. These pockmarks are relatively large, with the majority having a rough diameter between 100 and 200 m and an average internal depth of 15 m. Pockmarks along the Aquitaine slope are divided into subcircular (12%) and mostly elongated (88%) pockmarks including some coalescent. The slope and the coalescence of pockmarks, as the primary controlling factor, only constrains the elongation of part of the pockmarks. But the majority of elongated pockmarks are not aligned along the present-day prevailing current direction as it is the case across other continental shelves and slopes (Bøe et al., 1998; Schattner et al., 2016; Tallobre et al., 2016). Pockmarks along the Aquitaine slope are not randomly distributed with regards to the water depth and surrounding morphology. Slope-indenting submarine canyons are pockmark free zones as observed along, e.g., shelf-indenting canyons (Brothers et al., 2014). In the north of the studied area, pockmarks are constrained by the east–west oriented inter-canyon morphology while in the southern area, they are generally oriented NNE–SSW along the direction of the crests and inter-crests from the sediment wave system. There is no positive correlation between the dimension of the pockmark and water depths as has been observed elsewhere (Gafeira et al., 2012; Schattner et al., 2016). Instead, the pockmark size appears more often influenced by the nature and thickness of sediments (Baltzer et al., 2014; King and MacLean, 1970; Rise et al., 2015) than the water depth. Along the Aquitaine continental slope, the thickness of the upper most sedimentary layer, the unit U4 as defined by Faugères et al. (2002) and Gonthier et al. (2006), appears indeed to drive the occurrence of pockmarks. Thus, the pockmark distribution is sedimentologically controlled by (1) the presence and the thickness of the uppermost sedimentary cover, which is a few metres to a few tens of metre-thick, with (2) a secondary influence of inherited sedimentary structures such as the sediment waves.

The history of the Aquitaine slope pockmarks is recent with regards to the Aquitaine margin history and can be described as three main stages. Fluid migration from a shallow source level, a few metres to a few tens of metres below the present-day seafloor, and fluid expulsion at the seabed have led to the formation of circular pockmarks. These pockmarks were initiated not before the Holocene times, and possibly within the last 10 kyr. These pockmarks were most likely formed by past short-duration fluid-release events associated with microbial gas (methane) or possibly water without major associated diagenesis, as methane-derived authigenic carbonate precipitation. Then, near-bottom currents, different in orientation and velocity than present-day ones, have modified the pockmarks from circular to elongated ones in the WNW–ESE direction. This was possibly followed by a second but minor formation of pockmarks unless the 12% of subcircular pockmarks are former elongated ones that were modified later on by sediment infilling or collapse. At present-day, the Aquitaine slope is dominated by weaker near-bottom currents that may induce upwelling within the inactive pockmarks, contributing to the maintenance of their shape as proposed, observed and modelled for other studied cases (Brothers et al., 2011; Hammer et al., 2009; Pau et al., 2014).

Acknowledgments

The GAZCOGNE study, the marine expedition GAZCOGNE1 (https://doi.org/10.17600/13020070) and the PhD thesis of Guillaume Michel were co-funded by TOTAL and IFREMER as part of the PAMELA (https://doi.org/10.18142/236) (Passive Margin Exploration Laboratories) scientific project. The BOBGEO2 (https://doi.org/10.17600/10020020) marine expedition was part of the FP7 EU Project CORALFISH. The ASPEX2010A survey (https://doi.org/10.17600/10020010) was part of the EPIGRAM project. The authors wish to thank Johan Saout, Charline Guérin, Cécile Breton, Émeric Gautier, Élodie Petit, Romain Biville, and André Ogor for their contribution to data processing, Joana Gafeira for discussions on pockmark detection, Alison Chalm and Ewan Harney for English correction, and the two reviewers, Hervé Gillet and Soledad Garcia-Gil, for their helpful comments.

Appendix A. Supplementary data

Supplementary data associated with this article can be found, in the online version, at https://doi.org/10.1016/j.crte.2017.10.003.

References

Andresen, K.J., Huuse, M., Clausen, O.R., 2008. Morphology and distribution of Oligocene and Miocene pockmarks in the Danish North Sea-implications for bottom current activity and fluid migration. Basin Res. 20, 445–466, http://dx.doi.org/10.1111/j.1365-2117.2008.00362.x.

Baltzer, A., Ehrhold, A., Rigolet, C., Souron, A., Cordier, C., Clouet, H., Dubois, S.F., 2014. Geophysical exploration of an active pockmark field in the Bay of Concarneau, southern Brittany, and implications for resident suspension feeders. Geo-Marine Lett. 34, 215–230, http://dx.doi.org/10.1007/s00367-014-0368-0.

Batifoulier, F., Lazure, P., Bonneton, P., 2012. Poleward coastal jets induced by westerlies in the Bay of Biscay. J. Geophys. Res. Ocean. 117, 1–19, http://dx.doi.org/10.1029/2011JC007658.

Baudon, C., Gillet, H., Cremer, M., 2013. Focused fluid-flow processes through high-quality bathymetric, 2D seismic and Chirp data from the southern parts of the Bay of Biscay, France. In: EGU General Assembly Conference Abstracts. 763.

Bayon, G., Loncke, L., Dupré, S., Caprais, J.C., Ducassou, E., Duperron, S., Etoubleau, J., Foucher, J.-P., Fouquet, Y., Gontharet, S., Henderson, G.M., Huguen, C., Klaucke, I., Mascle, J., Migeon, S., Olu-Le Roy, K., Ondréas, H., Pierre, C., Sibuet, M., Stadnitskaia, A., Woodside, J., 2009. Multi-disciplinary investigation of fluid seepage on an unstable margin: The case of the Central Nile deep sea fan. Mar. Geol. 261, 92–104, http://dx.doi.org/10.1016/j.margeo.2008.10.008.

Biteau, J.-J., Le Marrec, A., Le Vot, M., Masset, J.-M., 2006. The Aquitaine Basin. Pet. Geosci. 12, 247–273, http://dx.doi.org/10.1144/1354-079305-674.

Bøe, R., Rise, L., Ottesen, D., 1998. Elongate depressions on the southern slope of the Norwegian Trench (Skagerrak): morphology and evolution. Mar. Geol. 146, 191–203, http://dx.doi.org/10.1016/S0025-3227(97)00133-3.

Brothers, D.S., Ruppel, C., Kluesner, J.W., Ten Brink, U.S., Chaytor, J.D., Hill, J.C., Andrews, B.D., Flores, C., 2014. Seabed fluid expulsion along the upper slope and outer shelf of the US Atlantic continental margin. Geophys. Res. Lett. 41, 96–101, http://dx.doi.org/10.1002/2013GL058048.

Brothers, L.L., Kelley, J.T., Belknap, D.F., Barnhardt, W.A., Andrews, B.D., Maynard, M.L., 2011. More than a century of bathymetric observations and present-day shallow sediment characterization in Belfast Bay, Maine, USA: implications for pockmark field longevity. Geo-Marine Lett. 31, 237–248, http://dx.doi.org/10.1007/s00367-011-0228-0.

Charria, G., Lazure, P., Le Cann, B., Serpette, A., Reverdin, G., Louazel, S., Batifoulier, F., Dumas, F., Pichon, A., Morel, Y., 2013. Surface layer circulation derived from Lagrangian drifters in the Bay of Biscay. J. Mar. Syst. 109, S60–S76, http://dx.doi.org/10.1016/j.jmarsys.2011.09.015.

Cirac, P., Berne, S., Castaing, P., Weber, O., 2000. Processus de mise en place et d'évolution de la couverture sédimentaire superficielle de la plateforme nord-aquitaine. Oceanol. Acta 23, 663–686.

Dandapath, S., Chakraborty, B., Karisiddaiah, S.M., Menezes, A., Ranade, G., Fernandes, W., Naik, D.K., Prudhvi Raju, K.N., 2010. Morphology of pockmarks along the western continental margin of India: employing multibeam bathymetry and backscatter data. Mar. Pet. Geol. 27, 2107–2117, http://dx.doi.org/10.1016/j.marpetgeo.2010.09.005.

Davy, B., Pecher, I., Wood, R., Carter, L., Gohl, K., 2010. Gas escape features off New Zealand: Evidence of massive release of methane from hydrates. Geophys. Res. Lett. 37, 1–5, http://dx.doi.org/10.1029/2010GL045184.

Dupré, S., Berger, L., Le Bouffant, N., Scalabrin, C., Bourillet, J.-F., 2014a. Fluid emissions at the Aquitaine Shelf (Bay of Biscay, France): a biogenic origin or the expression of hydrocarbon leakage? Cont. Shelf Res. 88, 24–33, http://dx.doi.org/10.1016/j.csr.2014.07.004.

Dupré, S., Mascle, J., Foucher, J.-P., Harmegnies, F., Woodside, J., Pierre, C., 2014b. Warm brine lakes in craters of active mud volcanoes, Menes caldera off NW Egypt: evidence for deep-rooted thermogenic processes. Geo-Marine Lett. 34, 153–168, http://dx.doi.org/10.1007/s00367-014-0367-1.

Dupré, S., Scalabrin, C., Grall, C., Augustin, J.-M., Henry, P., Sengör, A.M., Görür, N., Çagatay, M.N., Géli, L., 2015. Tectonic and sedimentary controls on widespread gas emissions in the Sea of Marmara: Results from systematic, shipborne multibeam echo sounder water column imaging. J. Geophys. Res. Solid Earth 120, 2891–2912.

Dupré, S., Woodside, J., Klaucke, I., Mascle, J., Foucher, J.-P., 2010. Widespread active seepage activity on the Nile Deep Sea Fan (offshore Egypt) revealed by high-definition geophysical imagery. Mar. Geol. 275, 1–19, http://dx.doi.org/10.1016/j.margeo.2010.04.003.

Durrieu De Madron, X., Castaing, P., Nyffeler, F., Courp, T., 1999. Slope transport of suspended particulate matter on the Aquitanian margin of the Bay of Biscay. Deep. Res. Part II Top. Stud. Oceanogr. 46, 2003–2027, http://dx.doi.org/10.1016/S0967-0645(99)00053-3.

Faugères, J.-C., Gonthier, E., Mulder, T., Kenyon, N., Cirac, P., Griboulard, R., Berné, S., Lesuavé, R., 2002. Multi-process generated sediment waves on the Landes Plateau (Bay of Biscay, North Atlantic). Mar. Geol. 182, 279–302, http://dx.doi.org/10.1016/S0025-3227(01)00242-0.

Gafeira, J., Long, D., Diaz-Doce, D., 2012. Semi-automated characterisation of seabed pockmarks in the central North Sea. Near Surf. Geophys. 10, 303–315, http://dx.doi.org/10.3997/1873-0604.2012018.

Gay, A., Lopez, M., Berndt, C., Séranne, M., 2007. Geological controls on focused fluid flow associated with seafloor seeps in the Lower Congo Basin. Mar. Geol. 244, 68–92, http://dx.doi.org/10.1016/j.margeo.2007.06.003.

Gay, A., Lopez, M., Ondreas, H., Charlou, J.-L., Sermondadaz, G., Cochonat, P., 2006. Seafloor facies related to upward methane flux within a Giant Pockmark of the Lower Congo Basin. Mar. Geol. 226, 81–95, http://dx.doi.org/10.1016/j.margeo.2005.09.011.

Gillet, H., Cirac, P., Lagié, B., 2008. Pockmarks on the southern margin of the Capbreton Canyon (south-eastern Bay of Biscay). In: Borja, A. (Ed.), XI International Symposium on Oceanography of the Bay of Biscay, 3, "Revisa de Investgacion Marina", San Sebastian, pp. 90–91.

Gonthier, E., Cirac, P., Faugères, J.C., Gaudin, M., Cremer, M., Bourillet, J.-F., 2006. Instabilities and deformation in the sedimentary cover on the upper slope of the southern Aquitaine continental margin, north of the Capbreton canyon (Bay of Biscay). Sci. Mar. 70, 89–100, http://dx.doi.org/10.3989/scimar.2006.70s189.

Hammer, Ø., Webb, K.E., Depreiter, D., 2009. Numerical simulation of upwelling currents in pockmarks, and data from the Inner Oslofjord, Norway. Geo-Marine Lett. 29, 269–275, http://dx.doi.org/10.1007/s00367-009-0140-z.

Harrington, P.K., 1985. Formation of pockmarks by pore-water escape. Geo-Marine Lett. 5, 193–197.

Hovland, M., Heggland, R., De Vries, M.H., Tjelta, T.I., 2010. Unit-pockmarks and their potential significance for predicting fluid flow. Mar. Pet. Geol. 27, 1190–1199, http://dx.doi.org/10.1016/j.marpetgeo.2010.02.005.

Iglesias, J., Ercilla, G., García-Gil, S., Judd, A.G., 2010. Pockforms: An evaluation of pockmark-like seabed features on the Landes Plateau, Bay of Biscay. Geo-Marine Lett. 30, 207–219, http://dx.doi.org/10.1007/s00367-009-0182-2.

Josenhans, H.W., King, L.H., Fader, G.B., 1978. A side-scan sonar mosaic of pockmarks on the Scotian Shelf. Can. J. Earth Sci. 15, 831–840.

Judd, A., Hovland, M., 2007. Seabed fluid flow: the impact on geology, biology and the marine environment. Cambridge University Press, Cambridge239.

Judd, A.G., Hovland, M., 1992. The evidence of shallow gas in marine sediments. Cont. Shelf Res. 12, 1081–1095, http://dx.doi.org/10.1016/0278-4343(92)90070-Z.

Kersalé, M., Marie, L., Le Cann, B., Serpette, A., Lathuilière, C., Le Boyer, A., Rubio, A., Lazure, P., 2016. Poleward along-shore current pulses on the inner shelf of the Bay of Biscay. Estuar. Coast. Shelf Sci. 179, 155–171.

King, L.H., MacLean, B., 1970. Pockmarks on the Scotian Shelf. Bull. Geol. Soc. Am. 81, 3141–3148, http://dx.doi.org/10.1130/0016-7606.

Kuhnt, T., Howa, H., Schmidt, S., Marié, L., Schiebel, R., 2013. Flux dynamics of planktic foraminiferal tests in the south-eastern Bay of Biscay (Northeast Atlantic margin). J. Mar. Syst. 109, 169–181.

Lazure, P., Garnier, V., Dumas, F., Herry, C., Chifflet, M., 2009. Development of a hydrodynamic model of the Bay of Biscay, Validation of hydrology. Cont. Shelf Res. 29, 985–997.

Le Boyer, A., Charria, G., Le Cann, B., Lazure, P., Marié, L., 2013. Circulation on the shelf and the upper slope of the Bay of Biscay. Cont. Shelf Res. 55, 97–107, http://dx.doi.org/10.1016/j.csr.2013.01.006.

Michel, G., Dupré, S., Saout, J., Ehrhold, A., Guerin, C., Gautier, E., Breton, C., Bourillet, J.-F., Loubrieu, B., 2017. Pockmark morphological attributes at the Aquitaine slope, GAZCOGNE1 (2013) and BOBGEO2 (2010) marine expeditions. SEANOE Database, http://dx.doi.org/10.17882/48323.

Migniot, C., 1977. Action des courants, de la houle et du vent sur les sédiments. La Houille Blanche, 1, pp. 9–47.

Moss, J.L., Cartwright, J., Moore, R., 2012. Evidence for fluid migration following pockmark formation: examples from the Nile Deep Sea Fan. Mar. Geol. 303, 1–13, http://dx.doi.org/10.1016/j.margeo.2012.01.010.

Pau, M., Gisler, G., Hammer, Ø., 2014. Experimental investigation of the hydrodynamics in pockmarks using particle tracking velocimetry. Geo-Marine Lett. 34, 11–19, http://dx.doi.org/10.1007/s00367-013-0348-9.

Pau, M., Hammer, Ø., 2013. Sediment mapping and long-term monitoring of currents and sediment fluxes in pockmarks in the Oslofjord, Norway. Mar. Geol. 346, 262–273, http://dx.doi.org/10.1016/j.margeo.2013.09.012.

Pilcher, R., Argent, J., 2007. Mega-pockmarks and linear pockmark trains on the West African continental margin. Mar. Geol. 244, 15–32, http://dx.doi.org/10.1016/j.margeo.2007.05.002.

Pingree, R.D., Mardell, G.T., New, A.L., 1986. Propagation of internal tides from the upper slopes of the Bay of Biscay. Nature 321, 154–158, http://dx.doi.org/10.1038/321154a0.

Plaza-Faverola, A., Bünz, S., Mienert, J., 2011. Repeated fluid expulsion through sub-seabed chimneys offshore Norway in response to glacial cycles. Earth Planet. Sci. Lett. 305, 297–308.

Riboulot, V., Thomas, Y., Berné, S., Jouet, G., Cattaneo, A., 2014. Control of Quaternary sea-level changes on gas seeps. Geophys. Res. Lett. 41, 4970–4977.

Rise, L., Bellec, V.K., Chand, S., Bøe, R., 2015. Pockmarks in the southwestern Barents Sea and – Finnmark fjords. Nor. J. Geol. 94, 263–282.

Roca, E., Muñoz, J.A., Ferrer, O., Ellouz, N., 2011. The role of the Bay of Biscay Mesozoic extensional structure in the configuration of the Pyrenean orogen: constraints from the MARCONI deep seismic reflection survey. Tectonics 30, 1–33, http://dx.doi.org/10.1029/2010TC002735.

Schattner, U., Lazar, M., Souza, L.A.P., Ten Brink, U., Mahiques, M.M., 2016. Pockmark asymmetry and seafloor currents in the Santos Basin offshore Brazil. Geo-Marine Lett. 36, 457–464, http://dx.doi.org/10.1007/s00367-016-0468-0.

Schmidt, S., Howa, H., Diallo, A., Martin, J., Cremer, M., Duros, P., Fontanier, C., Deflandre, B., Metzger, E., Mulder, T., 2014. Recent sediment transport and deposition in the Cap-Ferret Canyon, South-East margin of Bay of Biscay. Deep Sea Res. Part II Top. Stud. Oceanogr. 104, 134–144.

Schmidt, S., Howa, H., Mouret, A., Lombard, F., Anschutz, P., Labeyrie, L., 2009. Particle fluxes and recent sediment accumulation on the Aquitanian margin of Bay of Biscay. Cont. Shelf Res. 29, 1044–1052.

Sibuet, J.-C., Monti, S., Loubrieu, B., Mazé, J.-P., Srivastava, S., 2004. Carte bathymétrique de l'Atlantique nord-est et du golfe de Gascogne: implications cinématiques. Bull. la Soc. Geol. Fr. Tome 175, 429–442.

Sultan, N., Marsset, B., Ker, S., Marsset, T., Voisset, M., Vernant, A.-M., Bayon, G., Cauquil, E., Adamy, J., Colliat, J.-L., 2010. Hydrate dissolution as a potential mechanism for pockmark formation in the Niger delta. J. Geophys. Res. Solid Earth 115, 33.

Tallobre, C., Loncke, L., Bassetti, M.A., Giresse, P., Bayon, G., Buscail, R., de Madron, X.D., Bourrin, F., Vanhaesebroucke, M., Sotin, C., 2016. Description of a contourite depositional system on the Demerara Plateau: results from geophysical data and sediment cores. Mar. Geol. 378, 56–73, http://dx.doi.org/10.1016/j.margeo.2016.01.003.

Van Aken, H.M., 2000. The hydrography of the mid-latitude Northeast Atlantic Ocean II: the intermediate water masses. Deep. Res. Part I Oceanogr. Res. Pap. 47, 789–824, http://dx.doi.org/10.1016/S0967-0637(99)00112-0.

Webb, K.E., Hammer, Ø., Lepland, A., Gray, J.S., 2009. Pockmarks in the inner Oslofjord, Norway. Geo-Marine Lett. 29, 111–124.

Whiticar, M.J., 2002. Diagenetic relationships of methanogenesis, nutrients, acoustic turbidity, pockmarks and freshwater seepages in Eckernförde Bay. Mar. Geol. 182, 29–53.

Winnock, E., 1973. Exposé succinct de l'évolution paléogéologique de l'Aquitaine. Bull. Soc. geol. France 7, 5–12.